Czech University of Life Sciences Prague

Faculty of Forestry and Wood Sciences

Department of Forest Ecology

Forest biomass mapping of Mount Cameroon National Park

Diploma thesis

Author: Bc. Ondřej Vostarek

Thesis supervisor: Ing. Martin Mikoláš, Ph.D.

Consultant: Ing. Volodymyr Trotsiuk, Ph.D.

2020

CZECH UNIVERSITY OF LIFE SCIENCES PRAGUE

Faculty of Forestry and Wood Sciences

DIPLOMA THESIS ASSIGNMENT

Bc. Ondřej Vostarek

Forestry Engineering
Tropical Forestry and Agroforestry

Thesis title

Forest biomass mapping of Mount Cameroon National Park

Objectives of thesis

1) To produce a map of aboveground biomass of Mount Cameroon National Park.

2) To examine a relationship between aboveground biomass and specific environmental conditions.

Methodology

1) Creation of map of aboveground biomass via combination of field and remote sensing data.

2) Analysis of relationship between aboveground biomass and data on environmental conditions.

The proposed extent of the thesis

40-60 pages

Keywords

aboveground biomass, biomass mapping, remote sensing, tropical forest, forest inventory

---

Recommended information sources

Avitabile V, Baccini A, Friedl MA, Schmullius C (2012). Capabilities and limitations of Landsat and land cover data for aboveground woody biomass estimation of Uganda. Remote Sensing of Environment, 117, 366–380.

Avitabile V, Herold M, Henry M, Schmullius C (2011). Mapping biomass with remote sensing: a comparison of methods for the case study of Uganda. Carbon Balance and Management, 6, 7.

Avitabile V, Herold M, Heuvelink G, Lewis SL, Phillips OL, Asner GP et al. (2016). An integrated pan-tropical biomass maps using multiple reference datasets. Global Change Biology, 22: 1406–1420. doi:10.1111/gcb.13139.

Baccini A, Goetz SJ, Walker WS et al. (2012). Estimated carbon dioxide emissions from tropical deforestation improved by carbon-density maps. Nature Climate Change, 2, 182–185.

Ge Y, Avitabile V, Heuvelink GBM, Wang J, Herold M (2014). Fusion of pan-tropical biomass maps using weighted averaging and regional calibration data. International Journal of Applied Earth Observation and Geoinformation, 31, 13–24.

Saatchi SS, Harris NL, Brown S et al. (2011). Benchmark map of forest carbon stocks in tropical regions across three continents. Proceedings of the National Academy of Sciences, 108, 9899–9904.

Santoro M, Beaudoin A, Beer C, Cartus O, Fransson JE, Hall RJ et al. (2015). Forest growing stock volume of the northern hemisphere: Spatially explicit estimates for 2010 derived from Envisat ASAR. Remote Sensing of Environment, 168, 316-334.

Expected date of thesis defence

2019/20 SS – FFWS

The Diploma Thesis Supervisor

Ing. Martin Mikoláš, Ph.D.

Supervising department

Department of Forest Ecology

Advisor of thesis

Ing. Volodymyr Trotsiuk, Ph.D.

Electronic approval: 10. 6. 2019

prof. Ing. Miroslav Svoboda, Ph.D.

Head of department

Electronic approval: 22. 2. 2020

prof. Ing. Róbert Marušák, PhD.

Dean

Prague on 12. 04. 2020

I declare that I have prepared my diploma thesis on the topic of Forest biomass mapping of Mount Cameroon National Park independently under the guidance of Ing. Martin Mikoláš, Ph.D. and used only the sources I list in the list of sources used. I am aware that by publishing the diploma thesis I agree with its publication according to Act No. 111/1998 Coll. on Higher Education Institutions, as amended, regardless of the outcome of its defence.

In Prague on.....

Ondřej Vostarek

Acknowledgements

I would like to thank Dr. Marek Svitok for substantial aid with forest aboveground biomass modelling and interpretation, Dr. Volodymyr Trotsiuk and Dr. Martin Mikoláš for overall guidance during preparation of the diploma theses, Dr. Michael Loomis and Mark MacAllister for providing the data on elephant presence and doc. Jiří Doležal for providing the structural data from field sampling on Mount Cameroon.

Abstract

Tropical rain forests are considered to play an important role in the global climate change mitigation, acting as a potential carbon sink. However, to assess their true contribution and develop appropriate management strategies an accurate information about forest biomass stocks and distribution is necessary. The forest aboveground biomass in Mount Cameroon National Park, a biodiversity hotspot hosting one of the remaining West African populations of African forest elephant (*Loxodonta cyclotis* Matschie, 1900), was estimated using generalized linear mixed effect modelling based on combination of field sampled data from permanent study plots, remotely sensed data from Landsat 8 OLI and Sentinel-1 satellites, and kernel home ranges derived from telemetric monitoring of four forest elephant individuals. The probability of forest elephant presence was found to be positively related to the forest aboveground biomass density and significantly improved the biomass prediction, suggesting the importance of local disturbance regime for forest aboveground biomass estimation, and implying the necessity of further research for understanding the complex relationship between forest elephants and aboveground biomass, which could be beneficial for the conservation of African forest elephants as well as for the accurate aboveground biomass estimation in Afrotropical forests.

keywords: forest aboveground biomass, *Loxodonta cyclotis*, remote sensing, tropical montane forest, Mount Cameroon

Content

List of figures and tables

Figures

Tables

1. Introduction

The deforestation and degradation of tropical forests is considered to significantly contribute to the increase of CO_2 emissions (van der Werf et al. 2009), however, it is hard to quantify due to uncertainties in estimation of both the forest biomass and its loss (Houghton 2005). According to the latest Global Forest Resources Assessment the rate of global forest area loss has slowed down since 1990 – in contrary the net forest loss in Africa is still increasing (FAO 2020), despite the fact that most of the tropical African countries have joined the Reducing Emissions from Deforestation and Forest Degradation (REDD+) program of United Nations Framework Convention on Climate Change (UNFCCC, 2020). One of possible reasons could be a fact that for successful implementation of REDD+ accurate estimation of forest biomass within country is necessary (Pelletier et al. 2011). This could be challenging especially in case of tropical mountain forests due to their high variability between individual mountains as well as within the range of one mountain slope (Proctor et al. 2007). The primary tropical forests covering south-western slope of Mount Cameroon are not an exception (Hořák et al. 2019). The area is generally considered as a biodiversity hotspot hosting various endemic species including one of the remaining populations of African forest elephants (*Loxodonta cyclotis* Matschie, 1900) and was declared a national park in 2009 (MFW 2014). The role of African forest elephants in tropical rainforests is not completely understood yet – they have been reported to positively affect carbon stocks in lowland primary forests of central Africa (Berzaghi et al. 2019), however, their impact on mountain tropical forests have not been fully described so far.

2. The aim of the thesis

The aim of this thesis is to estimate forest aboveground biomass (AGB) of Mount Cameroon National Park based on a combination of field and remotely sensed data. Further, to examine the variation of forest AGB along the altitudinal gradient with different browsing pressure from African forest elephant population. Specifically, the following questions are addressed: (a) How forest AGB of Mount Cameroon vary along the altitudinal gradients? (b) What is the impact of African forest elephants on forest AGB distribution? (c) Can forest AGB of Mount Cameroon be accurately predicted using remote sensing and advanced modelling?

3. Review

3. 1. Forest biomass estimation

Estimation of biomass in forest ecosystems is usually based on a field census data (Chave et al. 2014) with the biomass of an individual tree as a basic unit which is further extrapolated on larger spatial scale (Chave et al. 2004). The tree aboveground biomass can be determined by process of harvesting, drying and weighting of the tree, however, this approach is cost and labour demanding beside the fact that it leads to a destruction of the measured tree (Imani et al. 2017). To overcome these discrepancies, allometric models for biomass estimation are being developed from the destructively sampled datasets (eg. Brown et al 1989, Overman et al. 1994, Chave et al. 2005, Segura and Kanninen 2005, Chave et al. 2014). These models are based on the relationship between biomass of a tree and its individual measures. While the most important tree aboveground biomass predictor is diameter, tree height can significantly improve the allometric model performance (Chave et al. 2005, Feldpausch et al. 2011, Feldpausch et al., 2012). However, both these variables are suspect to measurement errors, especially in difficult conditions of tropical forests - accurate diameter measurement can be complicated by steep terrain slope or high tree buttresses (Chave et al. 2004) and height measurements are restrained due to tall and dense canopies (Larjavaara and Muller-Landau 2013). Where the height information is not available, it can be predicted based on the diameter-height relationship – in that case usage of site-specific height models is recommended due to variability of this relationship under different environmental conditions (Feldpausch et al. 2011, Chave et al. 2014, Imani et al. 2017). The inaccuracies related to diameter and height measurements could be avoided by utilising ground or airborne Light Detection and Ranging (LiDAR) data to obtain individual tree volume (Hildebrandt and Iost 2012). This approach is able to provide a good aboveground biomass estimates (Chave et al. 2014), however, its successful implementation is conditioned by availability of accurate species-specific wood density information in order to convert the tree volume to biomass (Sagang et al. 2018). Although the tree diameter and height measurement errors are contributing to the total error in forest biomass estimation, larger proportion of uncertainty is related to the choice of appropriate allometric model, mainly due to insufficient destructive sample sizes used for their calibration (Chave et al. 2004, Feldpausch et al. 2012). This is the reason why local allometric models are often overperformed by global pantropical

models (Chave 2014). These global pantropical models are not species-specific therefore they usually incorporate species-specific wood density in order to account for inter species variance (Chave et al. 2004, Chave et al. 2005). Obtaining a correct wood density information through field sampling can be challenging since it is varying also between different parts of an individual tree (Sagang et al. 2018), however, Flores and Coomes (2011) proved that the large size of Global wood density database (Zanne et al. 2009) makes it an useful source of information for accurate wood density estimation. Another great source of uncertainties in forest aboveground biomass estimation, linked with size of used sampling plots and their representativeness of the mapped area (Chave et al. 2004), could be partially overcome with inclusion of additional remote sensing data in the process of plot level aboveground biomass extrapolation (Lu et al. 2016).

3. 2. Remote sensing in forest biomass mapping

With the expand of technology and data availability remote sensing becomes a useful tool for ecological monitoring including forest aboveground biomass mapping (Lu et al. 2016, Young et al. 2017). Various models are being constructed linking the field census information to a remotely sensed data allowing for biomass predictions over large areas (eg. Blackard et al. 2008, Mitchard et al. 2011). Role of the field census data is crucial for calibration and evaluation of these models (Lu et al. 2016). On the other hand, there are many indices which can be derived from the remote sensing data (Lu et al. 2016) - the most recent based on LiDAR metrics (eg. Dubayah et al. 2010, García et al. 2010), however, due to data availability optical and radar (Radio Detection and Ranging) based datasets still prevail in large scale forest biomass mapping (Avitabile et al. 2012, Lu et al. 2012, Lu et al. 2016).

3. 2. 1. Optical sensors

Optical sensors are detecting the amount of solar radiation reflected from a specific surface (Patenoude et al. 2005, Lu et al. 2016). Depending on their construction, they are able to capture information about incoming radiation in one to ten (multispectral sensors) or tens to hundreds (hyperspectral sensors) of spectral bands, each characterized by a certain wavelength range within the visible, near and middle infrared part of the electromagnetic spectrum (Patenoude et al. 2005). The amount of radiation reflected within each band is related to physical properties of the studied

surface and based on the examination of this spectral profile different types of surfaces can be distinguished (Patenoude et al. 2005, Lu et al. 2016). In forest aboveground biomass mapping, data from multispectral sensors are usually utilized (Avitabile et al. 2012, Lu et al. 2012, Lu et al. 2016), even though the application of optical remote sensing data in forest biomass mapping could be challenging, especially in tropics, due to signal saturation in case of complex forest stands (Lu et al. 2012) and frequent cloud cover (Asner 2001). Nevertheless, the most commonly used remote sensing dataset for forest aboveground biomass estimation consists of multispectral images from Landsat program – one reason is the large temporal and global spatial coverage and data continuity (Williams et al., 2006, Avitabile et al. 2012, Lu et al. 2012, Young et al. 2017), however, important factor was also the decision to provide data under open-access policy (Woodcock et al. 2008).

3. 2. 2. Radar sensors

In contrary to optical sensors, radar is considered to be a tool of so called active remote sensing (Patenaude et al. 2005). Synthetic aperture radar (SAR) sensors are emitting their own signal with specified wavelength within microwave part of the electromagnetic spectrum and recording the signal features (ie. amplitude, polarization, and phase) after reflection from studied surface (Patenaude et al. 2005). Based on these features the physical structure and properties of surface can be determined (Lu et al. 2016). The major advantage of radar above optical sensors in forest aboveground biomass mapping is independency on weather conditions thanks to own source of signal with ability to penetrate clouds (Patenaude et al. 2005). Radar signal is also able to penetrate forest canopies which helps to reduce the signal saturation in case of dense canopy cover, however, this ability differs between individual bands (Kasischke et al. 1997, Patenaude et al. 2005). Civilian radars are operating with several bands (eg. C, L, P), while each band have a different wavelength and therefore also different properties concerning surface penetration – longer wavelengths can penetrate deeper into the canopy (Patenaude et al. 2005, Lu et al. 2016). Even though the long-waved L and P bands are considered better aboveground biomass predictors in case of forests with complex stand structure (Imhoff 1995, Kasischke et al. 1997), open-access C-band data from Sentinel-1 satellites are also being used for tropical forest biomass mapping (Berninger et al. 2018, Debastiani et

al. 2019, Nuthammachot et al. 2020) thanks to their high spatial resolution (20x20 m) and revisit frequency (Filipponi 2019).

3. 2. 3. Combination of multiple sensors

All types of remote sensing data have pros and cons related to the spectral, spatial, and temporal resolution and those should be considered when assessing usefulness of certain dataset in relation to studied problematic (Patenaude et al. 2005). To overcome disadvantages of individual types of remote sensing data, information from different sensors can be combined (Kellndorfer et al. 2010). In tropical forest aboveground biomass mapping has been proved that the importance of spectral response in comparison to information about structural characteristics vary with complexity of mapped forest stand - in case of relatively simple structural composition the spectral response predominates as an aboveground biomass predictor, while with more complex stand structure the importance of structural characteristics grows, and best results are obtained when both types of information are used together (Lu 2005).

3. 3. Elephants and their role in Afrotropical forests

According to the IUCN Red List of Threatened Species, African savanna elephant (*Loxodonta africana* Blumenbach, 1797) and African forest elephant (*Loxodonta cyclotis* Matschie, 1900) are treated as one species classified as vulnerable (Blanc 2008), however, there are studies suggesting that they should be rather considered as separate species based on differences in genetics end ecological behaviour (Roca et al. 2001, Roca et al. 2015, Berzaghi et al. 2019). Despite the conservation efforts overall elephant population in Africa is still decreasing, mainly due to poaching and habitat loss, with even more rapid decline observed in African forest elephant population (Maisels et al. 2013, Wittemeyer et al. 2014). The Mount Cameroon African forest elephant population is one of the small West African fragments usually located in isolated areas surrounded by agricultural land (MFW 2014, Breuer et al. 2016, Thouless et al. 2016). Nevertheless, the African forest elephants are still understudied in comparison with African savanna elephants (Poulsen et al. 2017, Berzaghi et al. 2019). It has been discovered that large portion of African forest elephant's diet consists of fruits (Short 1981, Morgan and Lee 2007), which in combination with their ability to move across long distances makes them one of the most important animal seed dispersers of Afrotropical forest tree species (Theuerkauf et al. 2000, Blake et al.

2009, Campos-Arceiz and Blake 2011). Some of these species are exclusively dispersed by elephants (Cochrane 2003, Beaune et al. 2013) and are showing adaptations to elephant dispersal such as large size, inconspicuous colour (eg. green, yellow, or brown) and distinctive odour (Short 1981), reflecting elephant's dichromatic vision and well-developed sense of smell (Cochrane 2003, Yokoyama et al. 2005, Campos-Arceiz and Blake 2011). African forest elephants also browse on young trees contributing to stand structural diversity by maintaining forest gaps (Short 1981), which also serves as place for social interactions (Fishlock and Lee 2013). Effects of this browsing can be similar to forest stand thinning – reduction of stem density allows the surviving trees to reach larger dimensions resulting in rise of total aboveground biomass stocks (Berzaghi et al. 2019). Whereas Afrotropical forests are reported to have higher aboveground biomass density but lower tree density and diversity per hectare in comparison to Neotropical forests, some studies are suggesting that the presence of African forest elephants could be the main distinctive factor (Lewis et al. 2013, Terborgh et al. 2015, Berzaghi et al. 2019).

4. Materials and methods

4. 1. Study area

Mount Cameroon is an active Hawaiian type volcano without a central caldera (Payton 1993, Proctor et al. 2007) located in the Gulf of Guinea. Reaching 4 095 m above sea level (a. s. l.), it is considered to be the highest peak in West Africa (Proctor et al. 2007, Hořák et al. 2019) with significant influence on local rainfall pattern (Payton 1993, Proctor et al. 2007). The mean annual rainfall along its south-western coastal hillside decreases with altitude from approximately 5 000 mm near sea level to 4 000 mm at 1 000 m a. s. l. and 3 000 mm above 2 000 m a. s. l., while the north-eastern hillside lies in a rain shadow (Payton 1993, Proctor et al. 2007). The mean monthly air temperature at sea level varies from 27 °C to 35 °C with the hottest period from March to April and declines with rate of ~0.6 °C for each 100 m increase in altitude (Payton 1993, Proctor et al. 2007). Dry season occurs between December and February however, humidity remains at 75 to 80 % thanks to a sustaining mist and cloud cover (Payton 1993, Proctor et al. 2007). Despite the amount of water input there are no permanent streams due to extremely permeable Andosol soils (Payton 1993, Proctor et al. 2007). In contrary to relatively similar soil conditions (Payton 1993), different

types of vegetation cover can be found along the altitudinal gradient, starting with tropical lowland rain forest (300 – 900 m a. s. l.) and spanning to montane cloud forest (above 1 600 m a. s. l.) (see Figure 1) and montane grassland (above 2 250 m a. s. l.), with a structurally different mixture of closed and open canopy areas in the mid-altitude (900 – 1 600 m a. s. l.) (see Figure 2) where the local population of African forest elephants occurs (Payton 1993, Hořák et al. 2019). The transition between montane cloud forest and montane grassland appears to be controlled by volcanic activity and fire (Payton 1993, Proctor et al. 2007).

Figure 1. Montane cloud forest Closed canopy stand at ~2 000 m a. s. l. without signs of elephant presence.

Figure 2. Open canopy patch Forest canopy gap in area with presence of elephants.

4. 2. Data collection

4. 2. 1. Permanent study plots

In total 96 circular plots with 40 m in diameter (~0.1256 ha) were established along the altitudinal gradient on the south-western hillside of the Mount Cameroon during the dry season (November - December) in years 2011, 2012 and 2013 (Hořák et al.

2019). The forested area of the hillside was divided into six altitudinal belts (350, 650, 1 100, 1 500, 1 850 and 2 200 m a. s. l.) with 16 plots located within each belt (see Figure 3) (Hořák et al. 2019). All trees with diameter at breast height (DBH, at 1.3 m) > 10 cm were tagged on each plot and their status (alive or dead), species, DBH and height were recorded (Hořák et al. 2019).

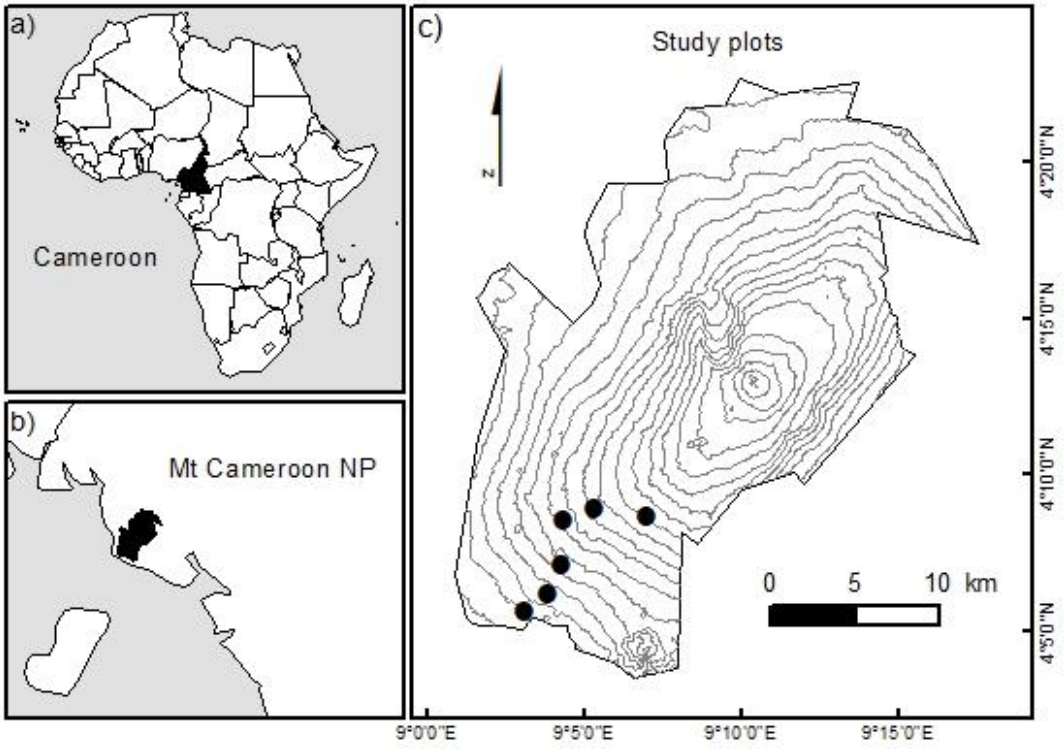

Figure 3. Study site Location of the Republic of Cameroon (a), Mount Cameroon National Park (b), and 96 permanent study plots on south-western hillside of Mount Cameroon (c), where each cluster of 16 plots is represented by one point. The digital elevation model was obtained from SRTM DEM (USGS 2014), the national park boundaries from The World Database on Protected Areas (UNEP-WCMC and IUCN 2020), and country boundaries from ArcGIS Online (drono_gSpace 2019).

4. 2. 2. Remote sensing data

The Landsat program was chosen as a source of multispectral satellite images due to the spatial and temporal coverage of the study area and spatial resolution which is close to the area of one sample plot (Fassnacht et al. 2014). Landsat 8 Operational Land Imager (OLI) Level-1 image from 10 January 2015 was selected being the closest image to the field sampling period with the lowest proportion of cloud cover in study area (Landsat 7 ETM+ images were excluded from examination because of the Scan Line Corrector failure, USGS 2003) and obtained through United States Geological Survey (USGS) Earth Explorer (USGS 2020) on 26 February 2020.

The synthetic-aperture radar (SAR) data were accessed via Copernicus Open Access Hub (ESA 2020) on 6 February 2020. A Sentinel-1 Level-1 Ground Range Detected dual polarisation (VV + VH) image acquired under Interferometric Wide swath mode on 12 April 2015 was chosen as an image of the study area with the closest sensing date in relation to the previously downloaded Landsat 8 OLI image.

4. 2. 3. Elephant population data

The information about African forest elephants on Mount Cameroon was obtained through ArcGIS Online from Map Package called Elephant Density Study, uploaded by Mark Macallister on 10 October 2012, and accessed via ArcGIS Desktop (ESRI 2019). The Map Package contains raster layers of kernel home ranges indicating the probability of an elephant presence in particular area (Dr. Michael Loomis, personal communication), based on data from satellite telemetric collars attached to 4 African forest elephant individuals, each one from a different herd (ARGOS 2020). These layers were exported, resampled to 30x30 m raster cell resolution using nearest neighbour algorithm and merged together summing the values in case of overlaps. Where no data were available, no elephant presence was assumed, represented by 0 probability value.

4. 3. Data processing

4. 3. 1. Plot level aboveground biomass calculation

The calculation of forest aboveground biomass on plot level was performed utilizing functions from BIOMASS R package (Rejou et al. 2017) using dataset of all measured living trees. In case of missing tree height record (56 from 5 223 trees), the height was estimated by ‘retrieveH’ function (Rejou et al. 2017) using Weibull height model (Bailey 1980, Feldpaush et al. 2012) based on the rest of the dataset. Taxonomy was cross-checked based on the information provided in The Plant List (The Plant List 2013) to match the taxonomy of the Global wood density database (Zanne et al. 2009) and checked for typos using ‘correctTaxo’ function (Rejou et al. 2017). Where it was possible, taxonomic information about family was retrieved with ‘getTaxonomy’ function (Rejout et al. 2017), in other cases the recorded family was used. Wood density was obtained with ‘getWoodDensity’ function (Rejou et al. 2017) averaging on species, genus or family level, depending on the available taxonomic information, and using data from the whole Global wood density database (Zanne 2009) according

to Flores and Coomes (2011). The utilization of Global wood density database (Zanne et al. 2009) should reduce the bias in individual tree aboveground biomass since the same dataset was also used for calibration of applied allometric model (Sagang et al. 2018). Since no local allometric model exist for the montane forests of Mount Cameroon (Loubota Panzou et al. 2016, Fayolle et al. 2018), the aboveground biomass on tree level was computed based on pantropical model developed by Chave et al. (2014):

$$AGB = 0.0673 \times (\rho D^2 H)^{0.976}$$

where D is diameter in cm, H is height in m and ρ is wood density in g cm^{-3}, implemented in 'AGBmonteCarlo' function (Rejou et al. 2017), which allows for the propagation of allometric model error. Additionally, errors of wood density estimation were included to the propagation represented by standard deviations from 'getWoodDensity' function (Rejou et al. 2017). The forest aboveground biomass on plot level was calculated as mean of 1000 iterations of 'AGBmonteCarlo' function (Rejou et al. 2017) divided by plotsize (0.1256 ha) in order to obtain aboveground biomass density in t ha^{-1}.

4. 3. 2. Landsat data transformation

The linear tasselled cap transformation (TCT) was used to compress the spectral information contained in Landsat 8 OLI bands into a few decorrelated variables (Baig et al. 2014). At first cloud mask based on Cloud and High Cloud Shadow Confidence layers of Quality Assessment band was created using QA Toolbox 1.3 (USGS 2017) in ArcGIS Desktop (ESRI 2019) and applied to individual spectral bands in order to exclude cloud-influenced pixels. In the next step spectral signal was converted from digital numbers (DN) to Top of Atmosphere Reflectance (TOA) according to Landsat 8 Data Users Handbook (USGS 2019) and transformed using coefficients from Baig et al. (2014) (see Table 1). The first three components of TCT (Brightness, Greenness and Wetness) are related to physical properties of the surface (Baig et al. 2014) and were chosen for further analysis as being reported to have a good correlation with tropical forest aboveground biomass (Lu et al. 2004).

Table 1. Tasselled cap coefficients for Landsat 8 OLI TOA reflectance Overtaken from Baig et al. (2014).

Landsat 8 TCT	Band 2 (Blue)	Band 3 (Green)	Band 4 (Red)	Band 5 (NIR)	Band 6 (SWIR1)	Band7 (SWIR2)
Brightness	0.3029	0.2786	0.4733	0.5599	0.5080	0.1872
Greenness	-0.2941	-0.2430	-0.5424	0.7276	0.0713	-0.1608
Wetness	0.1511	0.1973	0.3283	0.3407	-0.7117	-0.4559

4. 3. 3. Sentinel data pre-processing

The Sentinel-1 image was pre-processed in SNAP software (ESA 2018) according to a workflow described by Filipponi (2019). The orbit file was applied to improve the information about satellite position and velocity, thermal and border noise were removed, and backscatter was radiometrically calibrated to sigma nought values. Speckle noise was reduced by Refined Lee filtering and Range Doppler Terrain Correction was applied based on a SRTM 1Sec HGT DEM, in order to correct geometric distortions and project the image into Universal Transverse Mercator (UTM) coordinate system. During the projection cubic convolution resampling was used to obtain 30x30 m raster cell resolution to match the Landsat 8 OLI data. The corrected backscatter coefficient was converted to dB using a logarithmic transformation:

$$y = 10 \times \log_{10}|x|$$

where x is the unitless backscatter coefficient and y is the value in dB. Cross-polarized VH backscatter was used in further analysis since it is reported to be the most sensitive in terms of forest aboveground biomass detection (Kasischke et al. 1997).

4. 4. Aboveground biomass modelling

Generalized linear mixed effect model (GLMM) was used to predict aboveground biomass density while accounting for spatial autocorrelation inherent in the sampling design. Full GLMM was fitted by 'glmer' function from lme4 R package (Bates et al. 2015), using TCT components (Brightness, Greenness, Wetness), cross-polarized (VH) SAR backscatter, and elephant occurrence probability as fixed effect predictors, independent intercept for each plot cluster as random effect, and assuming normal

distribution of errors with logarithmic link function. Predictors for each plot were extracted from previously prepared raster layers (see Materials and methods – Elephant population data; Landsat data transformation; and Sentinel data pre-processing) based on plot coordinates with 20 m radius buffer to account for plot size, averaging values of all cells which centre falls within the buffer range. Thirteen plots, mostly from the highest altitudinal belt, had to be excluded from the analysis as spectral information was not available for them due to cloud cover. Additional one plot was identified as outlier based on Cook's distance. Excluding the observation considerably improved the model performance increasing conditional coefficient of determination (Nakagawa and Schielzeth 2013, Johnson 2014, Nakagawa et al. 2017) calculated by 'r.squaredGLMM' function from MuMIn R package (Bartón 2020) from ~0.21 to ~0.30. Therefore, it was decided to leave this plot out of the analysis, resulting in total number of 82 plots used for the final model calibration. Residuals of the GLMM were checked for presence of spatial autocorrelation using correlograms and no significant autocorrelation was observed.

4. 5. Aboveground biomass predicting

The final GLMM was used to predict the aboveground biomass of Mount Cameroon National Park based on previously prepared raster layers of remote sensed variables and elephant kernel home ranges (see Materials and methods – Elephant population data; Landsat data transformation; and Sentinel data pre-processing). To evaluate the results, predicted map was compared to Aboveground live woody biomass density map obtained from Global Forest Watch (WHRC unpublished data). This map contains the woody aboveground biomass densities (t ha^{-1}) of global forests in year 2000 at ~30 m spatial resolution and was created based on the methodology described in Baccini et al. (2012), using Landsat 7 Enhanced Thematic Mapper Plus (ETM+) top-of-atmosphere reflectance, tree canopy cover from the Global Forest Change version 1.2 dataset (Hansen et al. 2013), 1 arc-second SRTM V3 (Farr et al. 2007) and GTOPO30 (USGS 1996) altitude, and WorldClim climate data (Hijmans et al. 2005) as aboveground biomass predictors in random forest models calibrated on aboveground biomass densities estimated by allometric equations from a dataset of Geoscience Laser Altimeter System (GLAS) lidar-derived canopy metrics (WHRC unpublished data). The map was projected to Universal Transverse Mercator (UTM) coordinate system using nearest neighbour algorithm and soil mask based on Normalized

Difference Moisture Index (NDMI) (Kimes et al. 1981) calculated from Landsat 8 OLI Surface Reflectance product (Vermote et al. 2016) was applied during the comparison to exclude non-forested areas. The mask threshold was estimated by two-classes Natural Breaks (Jenks) classification algorithm in ArcGIS Desktop (ESRI 2019).

All calculations and data manipulations were performed in R 3.6.3 software (R Core Team 2020), unless stated otherwise, using packages rgdal (Bivand et al. 2019) and raster (Hijmans 2020) for spatial and raster operations.

5. Results

5. 1. Plot level aboveground biomass

The estimated forest aboveground biomass on plot level ranged from ~24 to ~1267 t ha^{-1} with mean value of ~418 t ha^{-1}, and varied across the altitudinal gradient with the lowest and the highest values present in 1500 and 1800 m a. s. l. altitudinal belts, respectively (see Figure 4).

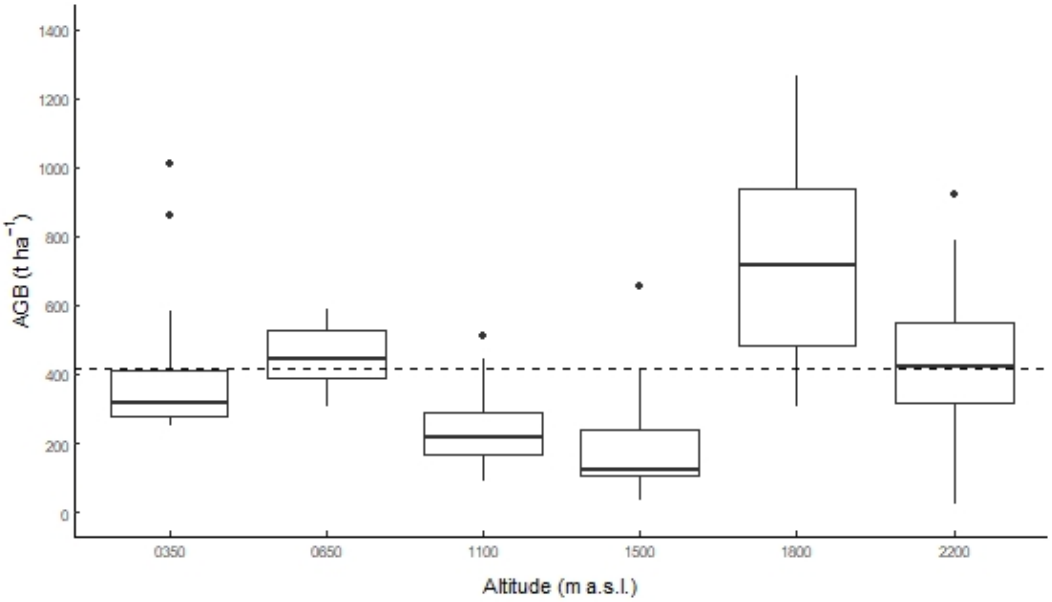

Figure 4. Aboveground biomass variation Plot level forest aboveground biomass values (t ha^{-1}) for 96 permanent sample plots are displayed according to plot location within altitudinal belt. Central line corresponds to median, lower, and upper hinges to first and third quartiles (25^{th} and 75^{th} percentiles), and whiskers extends from hinges to the smallest or largest value no further than 1.5 times the distance between first and third quartiles. Dashed line indicates the overall mean plot level forest aboveground biomass value.

When looking on the general trends in plot level structural data, estimated forest aboveground biomass showed increase with increasing altitude, same as the basal area (m^2 ha^{-1}), in contrary to tree density (number of trees per ha) which decreased with increasing altitude (see Figure 5).

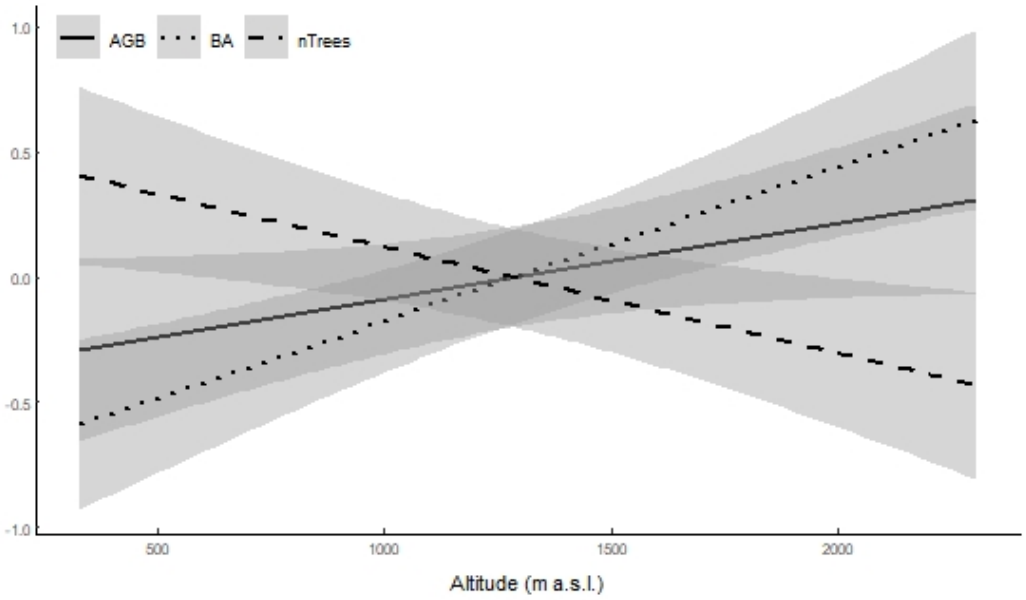

Figure 5. General trend in aboveground biomass, basal area, and tree stem density across the altitudinal gradient Linear regression fitted between altitude and scaled values of forest aboveground biomass (AGB), basal area (BA) and tree density (nTrees) on plot level. Values are displayed within 95 % confidence interval.

Concerning the species composition, contribution of individual genera to the total forest aboveground biomass differed between altitudinal belts with *Crudia* contributing the most in lower and *Schefflera* in upper altitudes (see Figure 6).

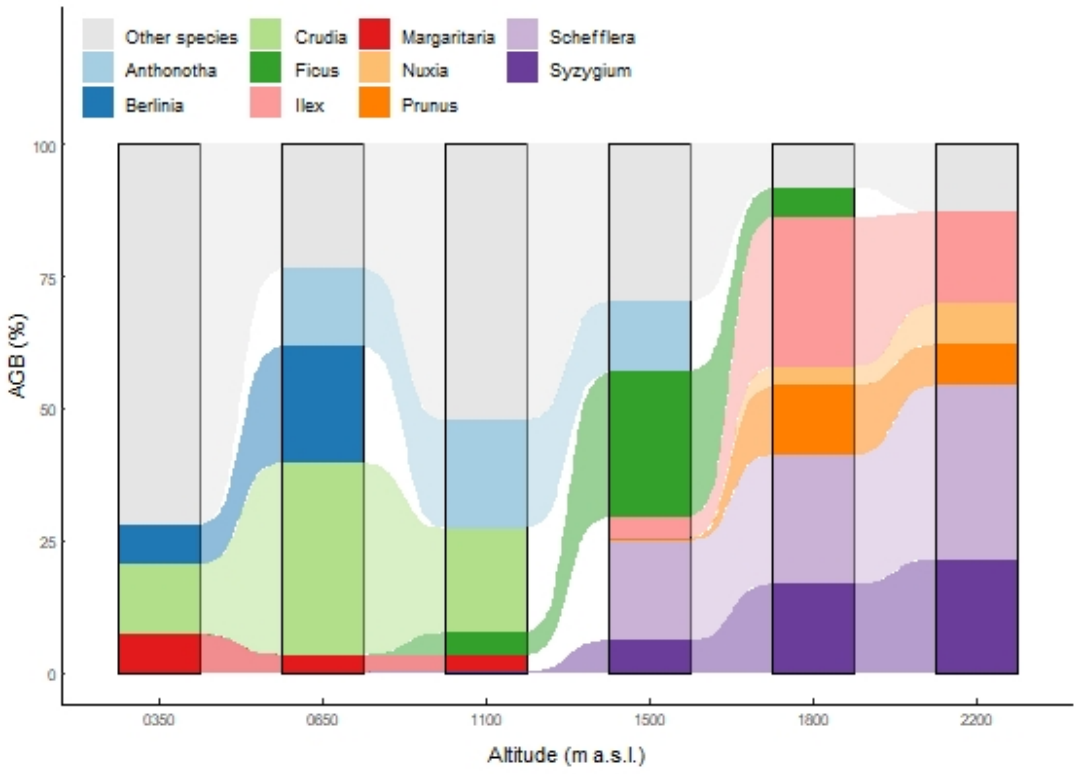

Figure 6. Aboveground biomass contribution Ten species contributing the most to the total forest aboveground biomass (AGB) of all measured plots are displayed according to their relative contribution to the total forest aboveground biomass (AGB) in individual altitude belts.

5. 2. Aboveground biomass model

The final GLMM had indicated significant positive effect of elephant presence on estimated aboveground biomass and significant negative relationship between forest aboveground biomass and Brightness tasselled cap component (see Table 2).

Table 2. Fixed effects evaluation Estimated coefficients of fixed effect predictors (VH – cross-polarized SAR backscatter, BR – Brightness, GR – Greenness, WT – Wetness, E – elephant occurrence probability). Significant estimations are marked with * ($\alpha \leq 0.05$) or ** ($\alpha \leq 0.001$), respectively.

Estimated coefficients				
VH	BR	GR	WT	E
-0.0084 ± 0.03	-6.7023 ± 3.17 *	10.6618 ± 5.91	-5.3771 ± 6.98	0.0399 ± 0.01 **

5. 3. Aboveground biomass prediction

The forest aboveground biomass densities predicted from GLMM have wider distribution in comparison to data obtained from Aboveground live woody biomass density map (WHRC unpublished data) (see Figure 7), and are shifted towards higher aboveground biomass density values, with mean of 484 t ha^{-1} and median of 429 t ha^{-1} compared to 241 t ha^{-1} and 235 t ha^{-1}, respectively.

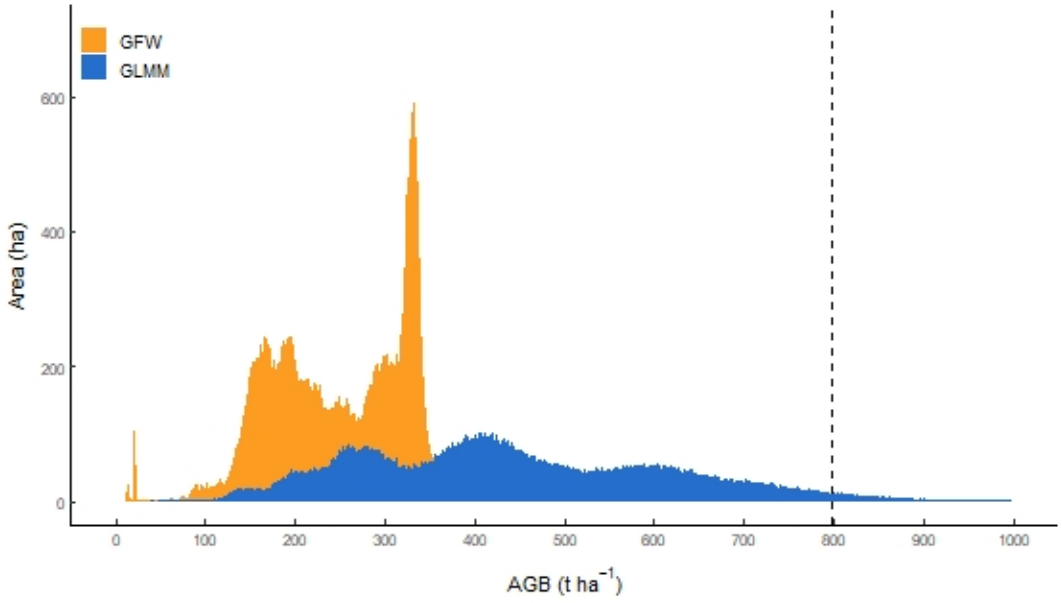

Figure 7. Aboveground biomass estimates comparison Mt Cameroon NP forest aboveground biomass density estimates (t ha^{-1}) in relation to area covered (ha). Data from Aboveground live woody biomass density map obtained from Global Forest Watch (WHRC unpublished data) are compared to aboveground biomass density values predicted from GLMM. Dashed line indicates the 95th percentile of predicted data (797.1109).

When comparing the aboveground biomass estimates with data from the 82 permanent study plots used to fit the GLMM, values obtained from Aboveground live woody biomass density map (WHRC unpublished data) seems to underestimate the plot level forest aboveground biomass with root mean square error (RMSE) of 305 t ha^{-1} and Pearson's r^2 of 0.24, while GLMM predictions appears to be more accurate with RMSE of 274 t ha^{-1} and Pearson's r^2 of 0.39 (see Figure 8).

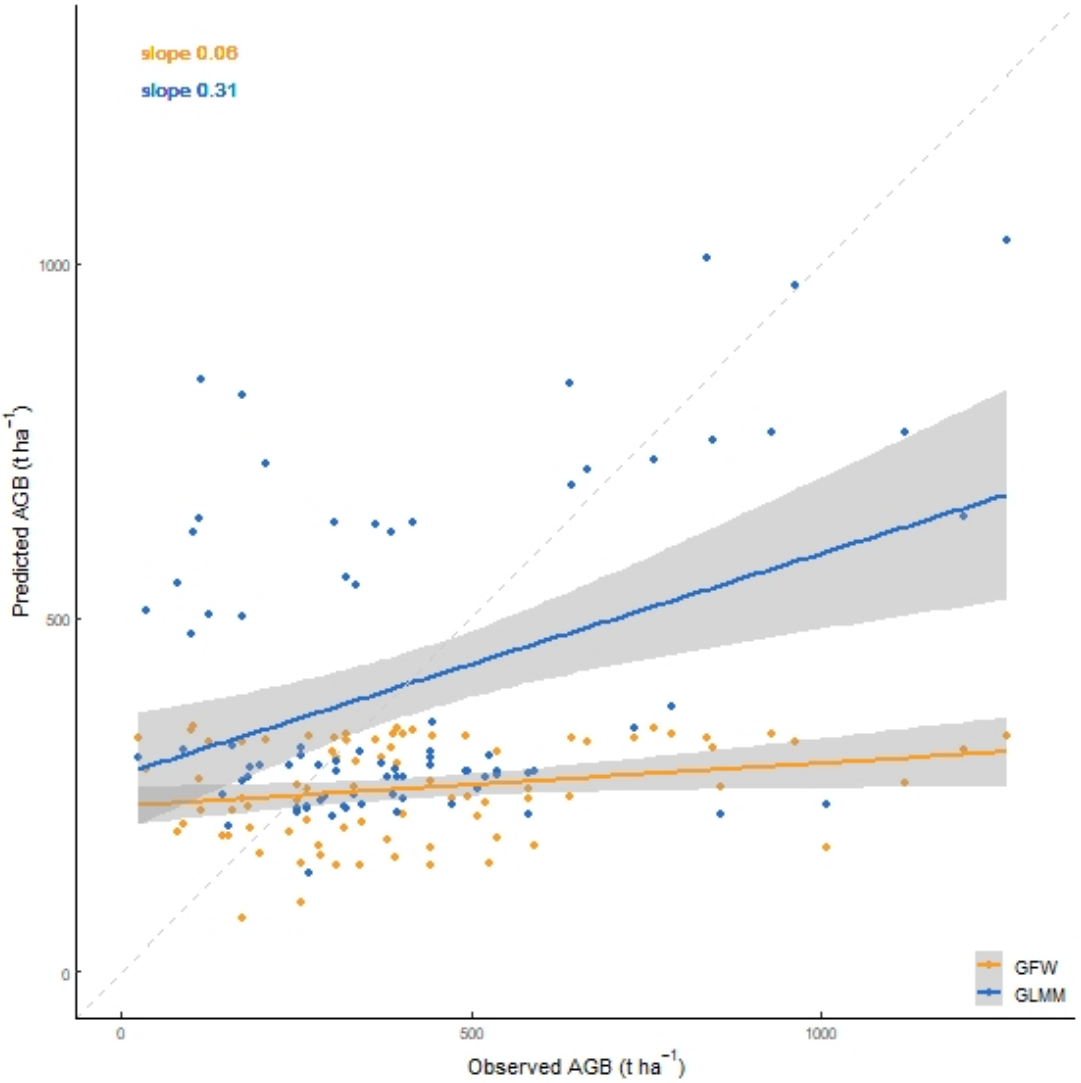

Figure 8. Aboveground biomass estimation Densities of forest aboveground biomass (t ha^{-1}) obtained from Aboveground live woody biomass density map (WHRC unpublished data) and predicted by GLMM are compared to observed aboveground biomass values (t ha^{-1}) from the 82 permanent study plots used for GLMM calibration.

Looking at the spatial distribution of aboveground biomass both datasets predict the highest values in an altitudinal range from approximately 1 400 to 2 200 m a. s. l. (see Figure 9), however, the GLMM tends to overestimate the aboveground biomass density in case of high probability of elephant presence, with maximal values ranging to ~16 530 t ha^{-1}.

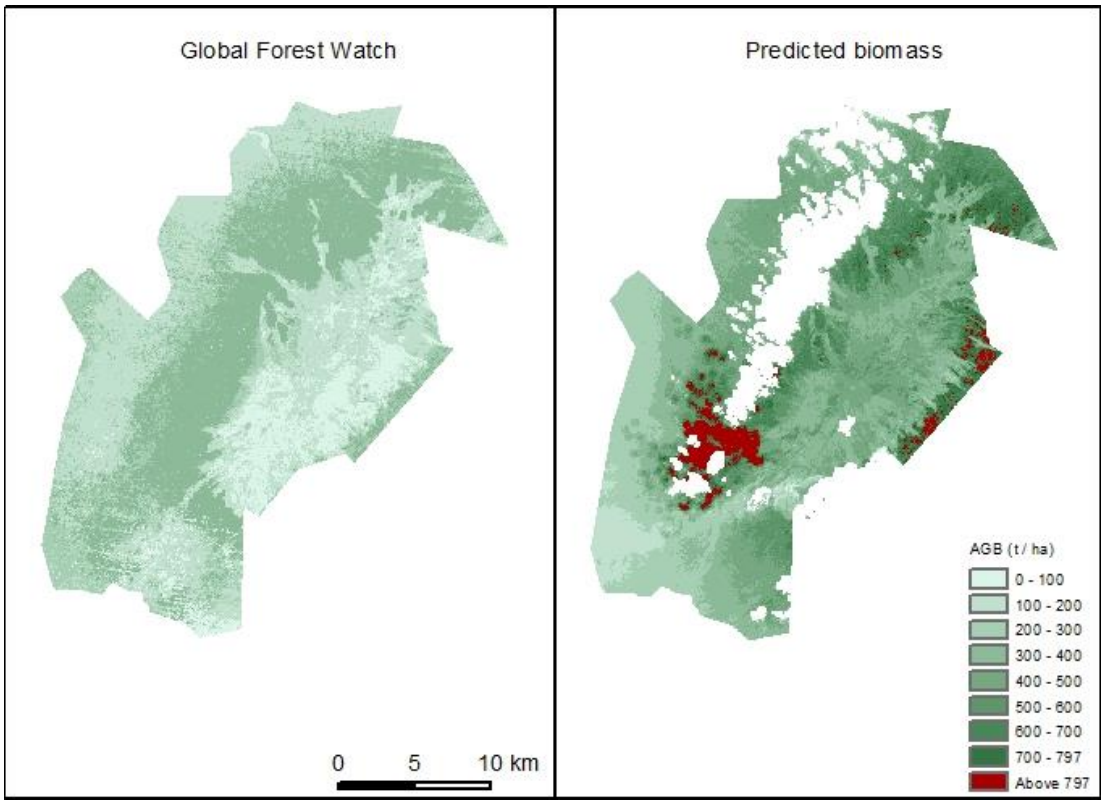

Figure 9. Aboveground biomass spatial distribution Estimation of Mt Cameroon NP forest aboveground biomass density (t ha^{-1}) based on Aboveground live woody biomass density map obtained from Global Forest Watch (WHRC unpublished data) and data predicted from GLMM. Red colour indicates values above the 95th percentile (797.1109), white missing satellite data due to cloud cover. Contains modified data from Copernicus Sentinel, Landsat, and The World Database on Protected Areas (UNEP-WCMC and IUCN 2020).

6. Discussion

6. 1. Altitudinal pattern of aboveground biomass

The increase of forest aboveground biomass on plot level with rising altitude is in contrary to majority of previous findings on forest aboveground biomass distribution across altitudinal gradients in tropical montane forests (Aiba and Kitayama 1999, Kitayama and Aiba 2002, Leuschner et al. 2007, Girardin et al. 2014, but see Alves et al. 2010). The generally observed lower forest aboveground biomass densities in higher altitudes of tropical mountains are being explained by reduction of tree growth driven by decreasing temperature, limiting amount of available soil nutrients, particularly N and P, or oxygen deficiency related to soil waterlogging (Tanner et al. 1998, Aiba and Kitayama 1999, Kitayama and Aiba 2002, Leuschner et al. 2007). While the effect of temperature was not tested in this thesis due to the lack of data with necessary spatial resolution, the volcanic soils on Mount Cameroon are well permeable and no limits in nutrients were found with the increasing altitude (Payton 1993, Proctor 2007), suggesting that different factors could influence the forest structure and

aboveground biomass distribution. It is possible that the lower forest aboveground biomass densities in the first altitudinal belt (350 m a. s. l.) are result of human disturbance (Alves et al. 2010), since the Mount Cameroon National Park is surrounded by about forty villages (MFW 2014), however, after increase in 650 m a. s. l. altitudinal belt the forest aboveground biomass density decreases again until a dramatic shift between the 1 500 and 1 800 m a. s. l. altitudinal belts (see Figure 4). When looking at the trend of basal area (m^2 ha^{-1}) and number of stems per hectare it also seems to be reverse than usual (Aiba and Kitayama 1999, Leuschner et al, 2007, Slik et al. 2010, Girardin et al. 2014) with larger basal area and lower stem density in higher altitudes indicating increase in tree size (see Figure 5). This change of forest structure is in agreement with findings of Payton (1993) and Proctor et al. (2007) and it is related to the forest aboveground biomass distribution through the important contribution of large trees in aboveground biomass stocks (Alves et al. 2010, Silk et al. 2010, Slik et al. 2013). One possible explanation of these reverse trends could be the occurrence of *Schefflera abyssinica* (Hochst. ex A.Rich.) Harms and *Schefflera mannii* (Hook.f.) Harms species, which were found on plots from 1 500 to 2 200 m a. s. l. altitudinal belt. These strangler species are able to grow up to large diameter dimensions and substantially influence the aboveground biomass in higher altitudinal belts (see Figure 6). The fact that the host of this strangler can be destroyed leaving a hollow in the centre of its diameter, combined with relatively small plotsize (~0.1256 ha), can lead to overestimation of forest aboveground biomass density on plots with high *Schefflera* spp. occurrence (Payton 1993, Chave et al. 2004). Exclusion of the *Schefflera* spp. from the plot level forest aboveground biomass estimation led to a decrease in total amounts of forest aboveground biomass densities, however, the overall pattern of forest aboveground biomass distribution along the altitudinal gradient remained the same, with the lowest and highest values in 1 500 and 1 800 m a. s. l., respectively, suggesting the general presence of larger trees in higher altitudes (data not shown). As majority of the studies describing opposite forest aboveground biomass, basal area, and tree stem density trends was conducted in Neotropical or Asian rainforests (Tanner et al. 1998, Aiba and Kitayama 1999, Kitayama and Aiba 2002, Leuschner et al. 2007, Slik et al. 2010, Girardin et al. 2014), the general difference in tropical forest structure between those continents, with Afrotropical forests having lower tree densities and higher basal area (Lewis et al. 2013, Slik et al.

2013, Treborgh et al. 2015), can be another explanation, possibly related to the presence of African forest elephants (Berzaghi et al. 2019).

6. 2. Effects of elephant population

When looking at the results shown by the final GLMM, the significant negative relationship between forest aboveground biomass and the Brightness tasselled cap component is in agreement with general interpretation of this component as representing the soil surface without vegetation cover (Baig et al. 2014). More interesting is the positive relationship found between forest aboveground biomass density and probability of African forest elephant presence, however, the model tends to overestimate the aboveground biomass in case of high elephant presence probability. This overestimation can be explained by extrapolating over the calibration values, since the probability of elephant presence on sampled study plots ranges from 0 to ~25 % , while the whole dataset range is from 0 to ~85 %, and suggests a non-linear relationship of elephant population presence and forest aboveground biomass. This relationship together with the positive impact of lower to moderate probability of elephant presence would be in agreement with findings from lowland Afrotropical forests, where moderate density of elephant population can promote the aboveground biomass through thinning effect while high elephant population densities leads to its decrease (Berzaghi et al. 2019). The positive relationship between elephant presence probability and forest aboveground biomass could be also interpreted in an opposite way, suggesting that forest elephants might seek areas with higher forest aboveground biomass, however, the habitat preferences may vary between individual elephants (Beirne et al. 2020), therefore larger dataset containing more individuals would be needed to test for this hypothesis. The African forest elephant presence probability has also been determined as more important aboveground biomass predictor in case of Mount Cameroon forests in comparison to common remote sensing variables, however, this can be partially due to the difficulties related with obtaining a good quality satellite data, resulting in a 2 to 4 years interval between the field sampling and satellite image acquisition. Despite the importance of African forest elephant presence as a forest aboveground biomass predictor, it can not fully explain the variability between the lowest and highest values in neighbouring 1 500 and 1 800 m a. s. l. altitudinal belts, since the mean probability of elephant presence on plots in those belts is quite similar – 14.3 and 14.1 %, respectively. Payton (1993) and Proctor et al. (2007)

suggested that the forest patchiness above the altitude of 1 100 m a. s. l. is a result of airfall deposits of volcanic ash and cinders, which overlays the present vegetation and fertile soil with layers of varying thickness influenced also by the local topography, creating random pattern of areas with hindered tree growth resulting in a mosaic of closed and open canopy forest with trees surviving the fall growing in large dimensions thanks to reduced competition. These forest canopy gaps can be further maintained by browsing of African forest elephants (Short 1981, Campbell 1991), who also use them as places for social interaction (Fishlock and Lee 2013), while the utilization of the closed canopy forest driven by their largely frugivorous diet (Short 1981, Theuerkauf et al. 2000) could reduce the tree stem density and promote growth of the large trees in the same time. This combined effect of African forest elephants and volcanic activity would be in agreement with results of model from Berzaghi et al. (2019), which supports the positive effect of forest elephants on aboveground biomass in closed canopy forest and suggests that the elephants can create large forest gaps on their own only under the highest population densities.

6. 3. Results of aboveground biomass mapping

Beside the overpredicted values, the overall higher forest aboveground biomass densities appears to be more adequate estimation than the data obtained from Aboveground live woody biomass density map (WHRC unpublished data) when compared with the range of forest aboveground biomass on plot level based on field sampling. This may be partly due to the fact that the year of resolution of the Aboveground live woody biomass density map is 2000 (WHRC unpublished data), therefore more than 10 years before the field sampling. While the Mount Cameroon was declared a national park in 2009 (MWF 2014), a positive trend in increase of forest aboveground biomass would be expected. Another possible explanation could be that despite the effort to select a site specific allometric equations and train continent specific predictive models during the process of development of the Aboveground live woody biomass density map (WHRC unpublished data), these were not able to capture the specific forest aboveground biomass distribution patterns on Mount Cameroon, while the usage of LiDAR-based aboveground biomass densities for calibration of models could also play a role in this case, providing less accurate estimates than ground-based measurements. This diversity of natural conditions implies the importance of local data-based mapping where high accuracy of forest aboveground

biomass estimation is necessary. Despite the fact that the predicted aboveground biomass densities seems to better reflect the permanent study plots estimates, the uncertainties connected with overestimation in case of high probability of elephant presence promotes the necessity of further research in order to improve the prediction accuracy. The results of the final GLMM indicates that the structural variability of Mount Cameroon forests (in this case represented by probability of elephant presence) is more important for aboveground biomass prediction than the spectral information, suggesting that incorporation of high-resolution structural measures – eg. airborne or unmanned aerial vehicle (UAV) LiDAR data – as a predictor in aboveground biomass modelling could result in more precise estimations.

7. Conclusion

The forest aboveground biomass distribution across the altitudinal gradient of Mount Cameroon was found to be atypical in comparison with other tropical mountains in terms of no clear relationship between the aboveground biomass and altitude. One of the possible factors influencing this distribution pattern could be the local population of African forest elephants, supported by results of the final GLMM which indicated a positive relationship between forest aboveground biomass and low to moderate probability of elephant presence, however, based on the available data it was not possible to decouple the effect of elephant population from influence of Mount Cameroon volcanic activity and further research is therefore needed in order to clarify the relationship between elephants and forest biomass. Understanding this relationship could on one hand improve our ecological knowledge about this vulnerable species and possibly help with the conservation of African forest elephant population, on the other hand it could be beneficial for the estimation of carbon storage in Afrotropical forests as it seems likely that inclusion of information about local disturbance regime could improve the prediction of forest aboveground biomass density and its spatial distribution.

References

Aiba SI, Kitayama K. 1999. Structure, composition and species diversity in an altitude-substrate matrix of rain forest tree communities on Mount Kinabalu, Borneo. *Plant Ecology* 140: 139-157.

Alves LF, Vieira SA, Scaranello MA, Camargo PB, Santos FAM, Joly CA, Martinelli LA. 2010. Forest structure and live aboveground biomass variation along an elevational gradient of tropical Atlantic moist forest (Brazil). *Forest Ecology and Management* 260: 679-691.

ARGOS. 2020. Animal tracking applications: Argos helps to define a protected area for elephants in Cameroon. Available at https://www.argos-system.org/elephants-cameroon/ [accessed 27 May 2020].

Asner GP. 2001. Cloud cover in Landsat observations of the Brazilian Amazon. *International Journal of Remote Sensing* 22: 3855-3862.

Avitabile V, Baccini A, Friedl MA, Schmullius Ch. 2012. Capabilities and limitations of Landsat and land cover data for aboveground woody biomass estimation of Uganda. *Remote Sensing of Environment* 117: 366-380.

Baccini A, Goetz SJ, Walker WS, Laporte NT, Sun M, Sulla-Menashe D, Hackler J, Beck PSA, Dubayah R, Friedl MA, Samanta S, Houghton RA. 2012. Estimated carbon dioxide emissions from tropical deforestation improved by carbon-density maps. *Nature Climate Change* 2: 182-185.

Baig MHA, Zhang L, Shuai T, Tong Q. 2014. Derivation of a tasselled cap transformation based on Landsat 8 at-satellite reflectance. *Remote Sensing Letters* 5: 423-431.

Bailey RL. 1980. The potential of Weibull-type functions as flexible growth curves: discussion. *Canadian Journal of Forest Research* 10: 117-118.

Bartón K. 2020. MuMIn: Multi-Model Inference. R package version 1.43.17. https://CRAN.R-project.org/package=MuMIn

Bates D, Maechler M, Bolker B, Walker S. 2015. Fitting Linear Mixed-Effects Models Using lme4. *Journal of Statistical Software* 67: 1-48. doi:10.18637/jss.v067.i01

Beaune D, Fruth B, Bollache L, Hohmann G, Bretagnolle F. 2013. Doom of the elephant-dependent trees in Congo tropical forest. *Forest Ecology and Management* 295: 109-117.

Beirne C, Meier AC, Brumagin G, Jasperse-Sjolander L, Lewis M, Masseloux J, Myers K, Fay M, Okouyi J, White LJT, Poulsen JR. 2020. Climatic and Resource Determinants of Forest Elephant Movements. *Frontiers in Ecology and Evolution* 8. https://doi.org/10.3389/fevo.2020.00096

Berninger A, Lohberger S, Stängel M, Siegert F. 2018. SAR-Based Estimation of Above-Ground Biomass and Its Changes in Tropical Forests of Kalimantan Using L- and C-Band. *Remote Sensing* 10: 831.

Berzaghi F, Longo M, Ciais P, Blake S, Bretagnolle F, Vieira S, Scaranello M, Scarascia-Mugnozza G, Doughty CE. 2019. Carbon stocks in central African forests enhanced by elephant disturbance. *Nature Geoscience* 12: 725-729.

Bivand R, Keitt T, Rowlingson B. 2019. rgdal: Bindings for the 'Geospatial' Data Abstraction Library. R package version 1.4-8. https://CRAN.R-project.org/package=rgdal

Blackard JA, Finco MV, Helmer EH, Holden GR, Hoppus ML, Jacobs DM, Lister AJ, Moisen GG, Nelson MD, Riemann R, Ruefenacht B, Salajanu D, Weyermann DL, Winterberg KC, Brandeis TJ, Czaplewski RL, McRoberts RE, Patterson PL, Tymcio RP. 2008. Mapping U.S. forest biomass using nationwide forest inventory data and moderate resolution information. *Remote Sensing of Environment* 112: 1658-1677.

Blake S, Deem SL, Mossimbo E, Maisels F, Walsh P. 2009. Forest Elephants: Tree Planters of the Congo. *Biotropica* 41: 459-468.

Blanc J. 2008. *Loxodonta africana. The IUCN Red List of Threatened Species* 2008: e.T12392A3339343. https://dx.doi.org/10.2305/IUCN.UK.2008.RLTS.T12392A3339343.en [accessed 22 May 2020].

Breuer T, Maisels F, Fishlock V. 2016. The consequences of poaching and anthropogenic change for forest elephants. *Conservation Biology* 30: 1019-1026.

Brown S, Gillespie AJR, Lugo AE. 1989. Biomass Estimation Methods for Tropical Forests with Applications to Forest Inventory Data. *Forest Science* 35: 881-902.

Campbell DG. 1991. Gap Formation in Tropical Forest Canopy by Elephants, Oveng, Gabon, Central Africa. *Biotropica* 23: 195-196.

Campos-Arceiz A, Blake S. 2011. Megagardeners of the forest – the role of elephants in seed dispersal. *Acta Oecologia* 37: 542-553.

Chave J, Andalo C, Brown S, Cairns MA, Chambers JQ, Eamus D, Fölster H, Fromard F, Higuchi N, Kira T, Lescure JP, Nelson BW, Ogawa H, Puig H, Riéra B, Yamakura T. 2005. Tree allometry and improved estimation of carbon stocks and balance in tropical forests. *Oecologia* 145: 87-99.

Chave J, Condit R, Aguilar S, Hernandez A, Lao S, Perez R. 2004. Error propagation and scaling for tropical forest biomass estimates. *Philosophical Transactions of the Royal Society of London. Series B: Biological Sciences* 359: 409-420.

Chave J, Réjou-Méchain M, Búrquez A, Chidumayo E, Colgan MS, Delitti WBC, Duque A, Eid T, Fearnside PM, Goodman RC, Henry M, Martínez-Yrízar A, Mugasha WA, Muller-Landau H, Mencuccini M, Nelson BW, Ngomanda A, Nogueira EM, Ortiz-Malavassi E, Pélissier R, Ploton P, Ryan CM, Saldarriaga JG, Vieilledent G. 2014. Improved allometric models to estimate the aboveground biomass of tropical trees. *Global Change Biology* 20: 3177-3190.

Cochrane EP. 2003. The need to be eaten: *Balanites wilsoniana* with and without elephant seed-dispersal. *Journal of Tropical Ecology* 19: 579-589.

Debastiani AB, Sanquetta CR, Corte APD, Rex FE, Pinto NS. 2019. Evaluating SAR-optical sensor fusion for aboveground biomass estimation in a Brazilian tropical forest. *Annals of Forest Research* 62: 109-122.

drono_gSpace. 2019. Africa_Countries. ArcGIS Feature Service available at https://services2.arcgis.com/aNJgWPqvZyTbm8FO/arcgis/rest/services/Africa_Countries/FeatureServer [accessed 5 June 2020].

Dubayah RO, Sheldon SL, Clark DB, Hofton MA, Blair JB, Hurtt GC, Chazdon RL. 2010. Estimation of tropical forest height and biomass dynamics using lidar remote sensing at La Selva, Costa Rica. *Journal of Geophysical Research* 115: G00E09.

ESA (European Space Agency). 2018. SNAP – Sentinel's Application Platform. Version 6.0.5. https://step.esa.int

ESA (European Space Agency). 2020. Copernicus Open Access Hub. Available at https://scihub.copernicus.eu/dhus/#/home [accessed 6 February 2020].

ESRI (Environmental Systems Research Institute). 2019. ArcGIS release 10.7. Redlands, CA.

FAO (Food and Agriculture Organization of the United Nations) (ed). 2020. *Global Forest Resources Assessment 2020 – Key findings*. Rome. https://doi.org/10.4060/ca8753en

Farr TG, Rosen PA, Caro E, Crippen R, Duren R, Hensley S, Kobrick M, Paller M, Rodriguez E, Roth L, Seal D, Shaffer S, Shimada J, Umland J, Werner M, Oskin M, Burbank D, Alsdorf D. 2007. The shuttle radar topography mission. *Reviews of geophysics* 45: RG2004.

Fassnacht FE, Hartig F, Latifi H, Berger C, Hernández J, Corvalán P, Koch B. 2014. Importance of sample size, data type and prediction method for remote sensing-based estimations of aboveground forest biomass. *Remote Sensing of Environment* 154: 102-114.

Fayolle A, Ngomanda A, Mbasi M, Barbier N, Bocko Y, Boyemba F, Couteron P, Fonton N, Kamdem N, Katembo J, Kondaoule HJ, Loumeto J, Maïdou HM, Mankou G, Mengui T, Mofack GII, Moundounga C, Moundounga Q, Nguimbous L, Nchama NN, Obiang D, Asue FOM, Picard N, Rossi V, Senguela YP, Sonké B, Viard L, Yongo OD, Zapfack L, Medjibe VP. 2018. A regional allometry for the Congo basin forests based on the largest ever destructive sampling. *Forest Ecology and Management* 430: 228-240.

Feldpausch TR, Banin L, Phillips OL, Baker TR, Lewis SL, Quesada CA, Affum-Baffoe K, Arets EJMM, Berry NJ, Bird M, Brondizio ES, de Camargo P, Chave J, Djagbletey G, Domingues TF, Drescher M, Fearnside PM, França MB, Fyllas NM, Lopez-Gonzalez G, Hladik A, Higuchi N, Hunter MO, Iida Y, Salim KA, Kassim AR, Keller M, Kemp J, King DA, Lovett JC, Marimon BS, Marimon-Junior BH, Lenza E, Marshall AR, Metcalfe DJ, Mitchard ETA, Moran EF, Nelson BW, Nilus R, Nogueira EM, Palace M, Patiño S, Peh KSH, Raventos MT, Reitsma JM, Saiz G, Schrodt F, Sonké B, Taedoumg HE, Tan S, White L, Wöll H, Lloyd J. 2011. Height-diameter allometry of tropical forest trees. *Biogeosciences* 8: 1081-1106.

Feldpausch TR, Lloyd J, Lewis SL, Brienen RJW, Gloor M, Monteagudo Mendoza A, Lopez-Gonzalez G, Banin L, Abu Salim K, Affum-Baffoe K, Alexiades M, Almeida S, Amaral I, Andrade A, Aragão LEOC, Araujo Murakami A, Arets

EJMM, Arroyo L, Aymard C GA, Baker TR, Bánki OS, Berry NJ, Cardozo N, Chave J, Comiskey JA, Alvarez E, de Oliveira A, Di Fiore A, Djagbletey G, Domingues TF, Erwin TL, Fearnside PM, França MB, Freitas MA, Higuchi N, Honorio C E, Iida Y, Jiménez E, Kassim AR, Killeen TJ, Laurance WF, Lovett JC, Malhi Y, Marimon BS, Marimon-Junior BH, Lenza E, Marshall AR, Mendoza C, Metcalfe DJ, Mitchard ETA, Neill DA, Nelson BW, Nilus R, Nogueira EM, Parada A, Peh KSH, Pena Cruz A, Peñuela MC, Pitman NCA, Prieto A, Quesada CA, Ramírez F, Ramírez-Angulo H, Reitsma JM, Rudas A, Saiz G, Salomão RP, Schwarz M, Silva N, Silva-Espejo JE, Silveira M, Sonké B, Stropp J, Taedoumg HE, Tan S, ter Steege H, Terborgh J, Torello-Raventos M, van der Heijden GMF, Vásquez R, Vilanova E, Vos VA, White L, Willcock S, Woell H, Phillips OL. 2012. Tree height integrated into pantropical forest biomass estimates. *Biogeosciences* 9: 3381-3403.

Filipponi F. 2019. Sentinel-1 GRD preprocessing workflow. *Multidisciplinary Digital Publishing Institute Proceedings* 18:11.

Fishlock V, Lee PC. 2013. Forest elephants: fission-fusion and social arenas. *Animal Behaviour* 85: 357-363.

Flores O, Coomes DA. 2011. Estimating the wood density of species for carbon stock assessments. *Methods in Ecology and Evolution* 2: 214-220.

García M, Riaño D, Chuvieco E, Danson FM. 2010. Estimating biomass carbon stocks for a Mediterranean forest in central Spain using LiDAR height and density data. *Remote Sensing of Environment* 114: 816-830.

Girardin CAJ, Farfan-Rios W, Garcia K, Feeley KJ, Jørgensen PM, Murakami AA, Pérez LC, Seidel R, Paniagua N, Claros AFF, Maldonado C, Silman M, Salinas N, Reynel C, Neill DA, Serrano M, Caballero C, de los Angeles La Torre Cuadros M, Macía MJ, Killeen TJ, Malhi Y. 2014. Spatial patterns of above-ground structure, biomass and composition in a network of six Andean elevation transects. *Plant Ecology & Diversity* 7: 161-171.

Hansen MC, Potapov PV, Moore R, Hancher M, Turubanova SA, Tyukavina A, Thau D, Stehman SV, Goetz SJ, Loveland TR, Kommareddy A, Egorov A, Chini L, Justice CO, Townshend JRG. 2013. High-resolution global maps of 21st-century forest cover change. *science* 342: 850-853.

Hijmans RJ, Cameron SE, Parra JL, Jones PG, Jarvis A. 2005. Very high resolution interpolated climate surfaces for global land areas. *International Journal of Climatology: A Journal of the Royal Meteorological Society* 25: 1965-1978.

Hijmans RJ. 2020. raster: Geographic Data Analysis and Modeling. R package version 3.0-12. https://CRAN.R-project.org/package=raster

Hildebrandt R, Iost A. 2012. From points to numbers: a database-driven approach to convert terrestrial LiDAR point clouds to tree volumes. *European Journal of Forest Research* 131: 1857-1867.

Hořák D, Ferenc M, Sedláček O, Motombi FN, Svoboda M, Altman J, Albrecht T, Nana ED, Janeček Š, Dančák M, Majeský L, Lltonga EN, Doležal J. 2019. Forest structure determines spatial changes in avian communities along an elevational gradient in tropical Africa. *Journal of Biogeography* 00: 1-13.

Houghton RA. 2005. Aboveground Forest Biomass and the Global Carbon Balance. *Global Change Biology* 11: 945-958.

Imani G, Boyemba F, Lewis S, Nabahungu NL, Calders K, Zapfack L, Riera B, Balegamire C, Cuni-Sanchez A. 2017. Height-diameter allometry and above ground biomass in tropical montane forests: Insights from the Albertine Rift in Africa. *PLoS ONE* 12: e0179653.

Imhoff ML. 1995. Radar Backscatter and Biomass Saturation: Ramifications for Global Biomass Inventory. *IEEE Transactions on Geoscience and Remote Sensing* 33: 511-518.

Johnson PCD. 2014. Extension of Nakagawa & Schielzeth's R_GLMM² to random slopes models. *Methods in Ecology and Evolution* 5: 44-946.

Kasischke ES, Melack JM, Dobson MC. 1997. The Use of Imaging Radars for Ecological Applications – A Review. *Remote Sensing Environment* 59: 141-156.

Kellndorfer JM, Walker WS, LaPoint E, Kirsch K, Bishop J, Fiske G. 2010. Statistical fusion of lidar, InSAR, and optical remote sensing data for forest stand height characterization: A regional-scale method based on LVIS, SRTM, Landsat ETM+, and ancillary data sets. *Journal of Geophysical Research* 115: G00E08.

Kimes DS, Markham BL, Tucker CJ. 1981. Temporal Relationships Between Spectral Response and Agronomic Variables of a Corn Canopy. *Remote Sensing of Environment* 11: 401-411.

Kitayama K, Aiba SI. 2002. Ecosystem structure and productivity of tropical rain forests along altitudinal gradients with contrasting soil phosphorus pools on Mount Kinabalu, Borneo. *Journal of Ecology* 90: 37-51.

Larjavaara M, Muller-Landau HC. 2013. Measuring tree height: a quantitative comparison of two common field methods in a moist tropical forest. *Methods in Ecology and Evolution* 4: 793-801.

Leuschner C, Moser G, Bertsch C, Röderstein M, Hertel D. 2007. Large altitudinal increase in tree root/shoot ratio in tropical mountain forests of Ecuador. *Basic and Applied Ecology* 8: 219-230.

Lewis SL, Sonké B, Sunderland T, Begne SK, Lopez-Gonzalez G, van der Heijden GMF, Phillips OL, Affum-Baffoe K, Baker TR, Banin L, Bastin JF, Beeckman H, Boeckx P, Bogaert J, De Cannière C, Chezeaux E, Clark CJ, Collins M, Djagbletey G, Djuikouo MNK, Droissart V, Doucet JL, Ewango CEN, Fauset S, Feldpausch TR, Foli EG, Gillet JF, Hamilton AC, Harris DJ, Hart TB, de Haulleville T, Hladik A, Hufkens K, Huygens D, Jeanmart P, Jeffrey KJ, Kearsley E, Leal ME, Lloyd J, Lovett JC, Makana JR, Malhi Y, Marshall AR, Ojo L, Peh KSH, Pickavance G, Poulsen JR, Reitsma JM, Sheil D, Simo M, Steppe K, Taedoumg HE, Talbot J, Taplin JRD, Taylor D, Thomas SC, Toirambe B, Verbeeck H, Vlemnickx J, White LJT, Willcock S, Woell H, Zemagho L. 2013. Above-ground biomass and structure of 260 African tropical forests. *Philosophical Transactions of the Royal Society B: Biological Sciences* 368: 20120295.

Loubota Panzou GJ, Doucet JL, Loumeto JJ, Biwole A, Bauwens S, Fayolle A. 2016. Biomasse et stocks de carbone des forêts tropicales africaines (synthèse bibliographique). *Biotechnologie, Agronomie, Société et Environnement* 20: 508-522.

Lu D. 2005. Aboveground biomass estimation using Landsat TM data in Brazilian Amazon. *International Journal of Remote Sensing* 26: 2509-2525.

Lu D, Chen Q, Wang G, Liu L, Li G, Moran E. 2016. A survey of remote sensing-based aboveground biomass estimation methods in forest ecosystems. *International Journal of Digital Earth* 9: 63-105.

Lu D, Chen Q, Wang G, Moran E, Batistella M, Zhang M, Laurin GV, Saah D. 2012. Aboveground Forest Biomass Estimation with Landsat and LiDAR Data and

Uncertainty Analysis of the Estimates. *International Journal of Forestry Research* 2012.

Lu D, Mausel P, Brondízio E, Moran E. 2004. Relationships between forest stand parameters and Landsat TM spectral responses in the Brazilian Amazon Basin. *Forest Ecology and Management* 198: 149-167.

Maisels F, Strindberg S, Blake S, Wittemeyer G, Hart J, Williamson EA, Aba'a R, Abitsi G, Ambahe RD, Amsini F, Bakabana PC, Hicks TC, Bayogo RE, Bechem M, Beyers RL, Bezangoye AN, Boundja P, Bout N, Akou ME, Bene Bene L, Fosso B, Greengrass E, Grossmann F, Ikamba-Nkulu C, Ilambu O, Inogwabini BI, Iyenguet F, Kiminou F, Kokangoye M, Kujirakwinja D, Latour S, Liengola I, Mackaya Q, Madidi J, Madzoke B, Makoumbou C, Malanda GA, Malonga R, Mbani O, Mbendzo VA, Ambassa E, Ekinde A, Mihindou Y, Morgan BJ, Motsaba P, Moukala G, Mounguengui A, Mowawa BS, Ndzai C, Nixon S, Nkumu P, Nzolani F, Pintea L, Plumptre A, Rainey H, de Semboli BB, Serckx A, Stokes E, Turkalo A, Vanleeuwe H, Vosper A, Warren Y. 2013. Devastating Decline of Forest Elephants in Central Africa. *PloS one* 8: e59469.

MFW (Ministry of Forestry and Wildlife). 2014. The management plan of Mount Cameroon National Park and its peripheral zone. Available at http://www.mtcameroonnationalpark.org/ManagingWithPeople.html#ManagementPlan [accessed 4 May 2020].

Mitchard ETA, Saatchi SS, Lewis SL, Feldpausch TR, Woodhouse IH, Sonké B, Rowland C, Meir P. 2011. Measuring biomass changes due to woody encroachment and deforestation/degradation in a forest-savanna boundary region of central Africa using multi-temporal L-band radar backscatter. *Remote Sensing of Environment* 115: 2861-2873.

Morgan BJ, Lee PC. 2007. Forest elephant group composition, frugivory and coastal use in the Réserve de Faune du Petit Loango, Gabon. *African Journal of Ecology* 45: 519-526.

Nakagawa S, Johnson PCD, Schielzeth H. 2017. The coefficient of determination R^2 and intra-class correlation coefficient from generalized linear mixed-effects models revisited and expanded. *Journal of the Royal Society Interface* 14: 20170213.

Nakagawa S, Schielzeth H. 2013. A general and simple method for obtaining R^2 from Generalized Linear Mixed-effects Models. *Methods in Ecology and Evolution* 4: 133–142.

Nuthammachot N, Askar A, Stratoulias D, Wicaksono P. 2020. Combined use of Sentinel-1 and Sentinel-2 data for improving above-ground biomass estimation. *Geocarto International*: 1-11.

Overman JPM, Witte HJL, Saldarriaga JG. 1994. Evaluation of regression models for above-ground biomass determination in Amazon rainforest. *Journal of Tropical Ecology* 10: 207-218.

Patenoude G, Milne R, Dawson TP. 2005. Synthesis of remote sensing approaches for forest carbon estimation: reporting to the Kyoto Protocol. *Environmental Science & Policy* 8: 161-178.

Payton RW. 1993. *Ecology, altitudinal zonation and conservation of tropical rain forests of Mount Cameroon*. Final project report R4600. Cranfield: Soil Survey and Land Research Centre.

Pelletier J, Ramankutty N, Potvin C. 2011. Diagnosing the uncertainty as detectability of emission reductions for REDD+ under current capabilities: an example for Panama. *Environmental Research Letters* 6: 024005.

Poulsen JR, Cooper R, Meier A, Mills E, Nuñez CL, Koerner SE, Blanchard E, Callejas J, Moore S, Sowers M. 2017. Ecological consequences of forest elephant declines for Afrotropical forests. *Conservation Biology* 32: 559-567.

Proctor J, Edwards ID, Payton RW, Nagy L. 2007. Zonation of forest vegetation and soils of Mount Cameroon, West Africa. *Plant Ecology* 192: 251-269.

R Core Team. 2020. R: A language and environment for statistical computing. R Foundation for Statistical Computing, Vienna, Austria. URL https://www.R-project.org

Réjou-Méchain M, Tanguy A, Piponiot C, Chave J, Hérault B. 2017. BIOMASS: an R package for estimating above-ground biomass and its uncertainty in tropical forests. *Methods in Ecology and Evolution* 8: 1163-1167.

Roca AL, Georgiadis N, Pecon-Slattery J, O'Brien SJ. 2001. Genetic Evidence for Two Species of Elephant in Africa. *Science* 293: 1473-1477.

Roca AL, Ishida Y, Brandt AL, Benjamin NR, Zhao K, Georgiadis NJ. 2015. Elephant Natural History: A Genomic Perspective. *Annual Review of Animal Biosciences* 3: 139-167.

Sagang LBT, Momo ST, Libalah MB, Rossi V, Fonton N, Mofack GII, Kamdem NG, Nguetsop VF, Sonké B, Pierre P, Barbier N. 2018. Using volume-weighted average wood specific gravity of trees reduces bias in aboveground biomass predictions from forest volume data. *Forest Ecology and Management* 424: 519-528.

Segura M, Kanninen M. 2005. Allometric Models for Tree Volume and Total Aboveground Biomass in a Tropical Humid Forest in Costa Rica. *Biotropica* 37: 2-8.

Short J, 1981. Diet and feeding behaviour of the forest elephant. *Mammalia* 45: 177-186.

Slik JWF, Aiba SI, Brearley FQ, Cannon CH, Forshed O, Kitayama K, Nagamasu H, Nilus R, Payne J, Paoli G, Poulsen AD, Raes N, Sheil D, Sidiyasa K, Suzuki E, van Valkenburg JLCH. 2010. Environmental correlates of tree biomass, basal area, wood specific gravity and stem density gradients in Borneo's tropical forests. *Global Ecology and Biogeography* 19: 50-60.

Slik JWF, Paoli G, McGuire K, Amaral I, Barroso J, Bastian M, Blanc L, Bongers F, Boundja P, Clark C, Collins M, Dauby G, Ding Y, Doucet JL, Eler E, Ferreira L, Forshed O, Fredriksson G, Gillet JF, Harris D, Leal M, Laumonier Y, Malhi Y, Mansor A, Martin E, Miyamoto K, Araujo-Murakami A, Nagamasu H, Nilus R, Nurtjahya E, Oliveira Á, Onrizal O, Parada-Gutierrez A, Permana A, Poorter L, Poulsen J, Ramirez-Angulo H, Reitsma J, Rovero F, Rozak A, Sheil D, Silva-Espejo J, Silveira M, Spironelo W, ter Steege H, Stevart T, Navarro-Aguilar GE, Sunderland T, Suzuki E, Tang J, Theilade I, van der Heijden G, van Valkenburg J, Do TV, Vilanova E, Vos V, Wich S, Wöll H, Yoneda T, Zang R, Zhang MG, Zweifel N. 2013. Large trees drive forest aboveground biomass variation in moist lowland forests across the tropics. *Global Ecology and Biogeography* 22: 1261-1271.

Tanner EVJ, Vitousek PM, Cuevas E. 1998. Experimental investigation of nutrient limitation of forest growth on wet tropical mountains. *Ecology* 79: 10-22.

Terborgh J, Davenport LC, Niangadouma R, Dimoto E, Mouandza JC, Schultz O, Jaen MR. 2015. The African rainforest: odd man out or megafaunal landscape? African and Amazonian forests compared. *Ecography* 39: 187-193.

The Plant List. 2013. Version 1.1. Available at http://www.theplantlist.org/ [accessed 3 November 2019].

Theuerkauf J, Waitkuwait WE, Guiro Y, Ellenberg H, Porembski S. 2000. Diet of forest elephants and their role in seed dispersal in the Bossematié Forest Reserve, Ivory Coast. *Mammalia* 64: 447-459.

Thouless CR, Dublin HT, Blanc JJ, Skinner DP, Daniel TE, Taylor RD, Maisels F, Frederick HL, Bouché P. 2016. African Elephant Status Report 2016: an update from the African Elephant Database. *Occasional Paper Series of the IUCN Species Survival Commission* 60.

UNEP-WCMC (United Nations Environment Programme World Conservation Monitoring Centre), IUCN (International Union for Conservation of Nature). 2020. Protected Planet: The World Database on Protected Areas (WDPA) [On-line]. Cambridge, UK: UNEP-WCMC and IUCN. Available at: www.protectedplanet.net [accessed 5 March 2020].

UNFCCC (United Nations Framework Convention on Climate Change). 2020. REDD+ web platform. Available at https://redd.unfcc.int [accessed 19 May 2020].

USGS (United States Geological Survey). 1996. Global 30 Arc-Second Elevation (GTOPO30). https://doi.org/10.5066/F7DF6PQS

USGS (United States Geological Survey) (ed). 2003. *Preliminary Assessment of the Value of Landsat 7 ETM+ Data following Scan Line Corrector Malfunction*. SD 57198. EROS Data Center, Sioux Falls.

USGS (United States Geological Survey). 2014. Shuttle Radar Topography Mission 1 Arc-Second Global. https://doi.org/10.5066/F7PR7TFT

USGS (United States Geological Survey). 2017. Landsat Quality Assessment ArcGIS Toolbox. U.S. Geological Survey software release. https://doi.org/10.5066/F7JM284N

USGS (United States Geological Survey) (ed). 2019. *Landsat 8 (L8) Data Users Handbook*. Version 5.0. LSDS-1574. EROS, Sioux Falls, South Dakota.

USGS (United States Geological Survey). 2020. Earth Explorer. Available at https://earthexplorer.usgs.gov [accessed 8 May 2020].

van der Werf GR, Morton DC, DeFries RS, Olivier JGJ, Kasibhatla PS, Jackson RB, Collatz GJ, Randerson JT. 2009. CO_2 emissions from forest loss. *Nature geoscience* 2: 737-738.

Vermote E, Justice C, Claverie M, Franch B. 2016. Preliminary analysis of the performance of the Landsat 8/OLI land surface reflectance product. *Remote Sensing of Environment* 185: 46-56.

WHRC (Woods Hole Research Center). Unpublished data. Aboveground live woody biomass density. Accessed through Global Forest Watch Climate. Available at http://data.globalforestwatch.org/datasets/8f93a6f94a414f9588ce4657a39c59ff_1 [accessed 27 May 2020].

Williams DL, Goward S, Arvidson T. 2006. Landsat: Yesterday, Today, and Tomorrow. *Photogrammetric Engineering & Remote Sensing* 72: 1171-1178.

Wittemeyer G, Northurp JM, Blanc J, Douglas-Hamilton I, Omondi P, Burnham KP. 2014. Illegal killing for ivory drives global decline in African elephants. *PNAS* 111: 13117-13121.

Woodcock CE, Allen R, Anderson M, Belward A, Bindschadler R, Cohen W, Gao F, Goward SN, Helder D, Helmer E, Nemani R, Oreopoulos L, Schott J, Thenkabail PS, Vermote EF, Vogelmann J, Wulder MA, Wynne R. 2008. Free Access to Landsat Imagery. *Science* 320: 1011-1011.

Yokoyama S, Takenaka N, Agnew DW, Shoshani J. 2005. Elephants and Human Color-Blind Deuteranopes Have Identical Sets of Visual Pigments. *Genetics* 170: 335-344.

Young NE, Anderson RS, Chignell SM, Vorster AG, Lawrence R, Evangelista PH. 2017. A survival guide to Landsat preprocessing. *Ecology* 98: 920-932.

Zanne AE, Lopez-Gonzalez G, Coomes DA, Ilic J, Jansen S, Lewis SL, Miller RB, Swenson NG, Wiemann MC, Chave J. 2009. Global wood density database. Dryad. https://doi.org/10.5061/dryad.234